Published in final edited form as:

Toxicol In Vitro. 2018 October ; 52: 251–254. doi:10.1016/j.tiv.2018.05.015.

Early assessment of burn severity in human tissue ex vivo with multi-wavelength spatial frequency domain imaging

Chien Poon[1], **Ulas Sunar**[1], **Daniel J. Rohrbach**[1], **Smita Krishnamurthy**[2,4,5], **Thomas Olsen**[2,6], **Michael Kent**[2,6], **Nathan M. Weir**[2], **Richard Simman**[2,3], and **Jeffrey B. Travers**[2,3,4,*]

[1]Department of Biomedical, Industrial & Human Factors Engineering, Wright State University, Dayton, OH, 45435, USA

[2]Department of Dermatology, Boonshoft School of Medicine, Wright State University, Dayton, OH, 45435, USA

[3]Department of Pharmacology & Toxicology, Boonshoft School of Medicine, Wright State University, Dayton, OH, 45435, USA

[4]Dayton Veterans Administration Medical Center, Dayton, OH, 45428, USA

[5]Department of Pathology & Laboratory Medicine, Boonshoft School of Medicine, Wright State University, Dayton, OH, 45435, USA

[6]Dermpathology Laboratory of Central States, Dayton, OH, 45459, USA

Abstract

Early knowledge about burn severity and depth can lead to improved outcome for patients. In this study, we investigated the change in optical properties in *ex vivo* human skin following thermal burn injuries. Human skin removed during body contouring procedures was subjected to thermal burn injury for either 10 or 60 seconds. Multi-wavelength spatial frequency domain imaging (SFDI) measurements were performed on each sample and the optical properties (absorption and scattering parameters) were obtained at each wavelength. Multi-wavelength fitting was used to quantify absorption and scattering parameters, and these parameters were compared to histologic assessments of burn depth related to burn severity. Our results indicated substantial changes in optical scattering parameters and these changes correlated well with the burn severity and depth, and fit closely with previously reported studies using porcine *in vivo* models. This study provides the characterization of thermal burn injury on human skin *ex vivo* by using the optical method of SFDI with high sensitivity and specificity. This preclinical human model system without live animals could have uses in testing the imaging parameters of other skin injuries, including from caustic agents.

[*]Correspondence: jeffrey.travers@wright.edu 3640 Colonel Glenn Highway, 207 Health Sciences, Dayton, OH, 45435 Tel.: +1-937-775-2463.

Compliance with Ethical Standards

Conflict of Interest: The authors declare that they have no conflict of interest.

Informed Consent: We used discarded de-identified skin so it was exempt.

Keywords

Thermal burn; human skin; animal testing alternatives; mesoscopic imaging

Introduction

Burns can be caused by many types of sources including heat, electricity, radiation, chemical agents, and friction (Tiwari, 2012). In the United States, the American Burn Association estimates that approximately 500,000 people seek treatment for burn injuries every year (Miller et al., 2008). Of those, about 45,000 have burns requiring medical treatment, and approximately 3,500 cases result in death.

Burn injuries are defined by the depth of the wound as superficial, deep partial, or full-thickness (Renz and Cancio, 2012). Superficial burns involve the most superficial layer of skin (the epidermis) only. These burns typically do not blister and epidermal regeneration can occur, leading to successful healing. Superficial partial-thickness burns involve the epidermis and some of the dermis. The basement layer typically remains intact and healing can occur. Deep partial-thickness burns damage the entire dermis and typically require debridement and skin grafting. Full-thickness burns cause damage through the entire dermis and down into the hypodermis (adipose layer) requiring debridement and skin grafts (Renz and Cancio, 2012). Although clinicians can readily diagnose superficial and full-thickness burns, the current challenge is classifying partial-thickness burns. Because of their ability to heal without treatment, superficial partial-thickness burns can be treated differently than deep partial-thickness burns, with the latter often needing skin grafting. Therefore, it is important to know the severity and depth of burn to determine the appropriate treatment.

Mesoscopic diffuse optical imaging techniques, such as laminar optical tomography (LOT) (Muldoon et al., 2012, Ozturk et al., 2016) and spatial frequency domain imaging (SFDI) (Rohrbach et al., 2014, 2015, Cuccia et al. 2009, Cuccia et al. 2005), are well suited for tissue characterization, providing structural and functional information with relatively high spatial resolution (several hundreds of microns) and depths of a few millimeters. Compared to LOT, SFDI is a wide-field, non-contact technique that provides quantitative maps of tissue optical properties, namely absorption and scattering parameters without the requirements of laser scanning (Cuccia et al., 2009, Cuccia et al., 2005). Multi-wavelength measurements of absorption and scattering allow quantification of blood related functional parameters such as tissue deoxy-, oxy- and total-hemoglobin concentrations, and oxygen saturation as well as tissue scattering parameters (Cuccia et al., 2009, Gioux et al., 2011). SFDI quantification of these parameters has demonstrated usefulness in burn wounds (Thatcher et al., 2016, Nguyen T.T. et al., 2013, Nguyen JQ et al., 2013, Ponticorvo et al., 2014). Mazhar and colleagues showed that SFDI quantification of physiological parameters can determine the severity of burn wounds in a pre-clinical porcine model (Mazhar et al., 2014). In this study we used a custom built SFDI system to image *ex vivo* human skin with superficial partial-thickness and deep partial-thickness burns, thereby investigated the ability of SFDI to predict thermal burn severity in human skin. We quantified absorption and scattering related parameters at multiple wavelengths to compare with histologic depth. These studies indicate

that SFDI can have uses in predicting thermal burn severity related to injury depth in human skin *ex vivo*, and compare favorably with published *in vivo* porcine studies (Mazhar et al., 2014).

Methods

Skin Preparation and Burn Model

Discarded de-identified abdominoplasty skin was obtained from plastic surgery and used within two hours of removal from the patient. The tissue was cut into three ~10 x10 cm squares. One sample was control (no burn) and two samples received burns. The burns were generated by heating metal blocks in boiling water (100°C) and placing them on the skin for a fixed amount of time (Figure 1a). One burn sample received 10-second burn by placing one metal block in contact with the skin surface for 10 seconds. The remaining sample received a 60-second burn by placing one metal block in contact with the skin for 30 seconds followed immediately by application of a second heated block in the same location for another 30 seconds. Skin samples were imaged within one hour of burns.

SFDI Instrumentation

An SFDI instrument (Figure 1b) was implemented similar to our previous work (Rohrbach et al., 2014, 2015). Briefly, the instrument consisted of four collimated light emitting diodes (LEDs) with center wavelengths of 490nm, 590nm, 660nm and 780nm (LCS series, Mightex, Toronto, Ontario, Canada) focused into a liquid light guide. The LEDs were sequentially selected with a four-channel LED controller (SLC-SA04-US, Mightex, Toronto, Ontario, Canada) so only one wavelength was on at a time. The liquid light guide relayed the selected wavelength to a digital micromirror device (DMD) having 1024 × 728 pixel resolution (DLP LightCrafter 4500, Texas Instruments, Dallas, TX). Sine wave patterns were sent to the DMD with 11 different frequencies ranging from 0 to 0.44 mm^{-1}, with three phases (0, $2\pi/3$, $4\pi/3$) for each frequency. A lens projected the patterns onto the tissue surface and a camera lens collected the reflected light and relayed the image to a camera (Zyla, Andor Technology, Belfast, United Kingdom). A 3-D printed light shield with an imaging window blocked room light and ensured that the tissue samples were always at the focal plane of the camera and DMD. Both the camera and DMD were focused on the same field of view, within the imaging window of the light shield. A custom LabView (National Instruments, Austin, TX) program allowed the LED current and camera exposure times to be adjusted.

SFDI Measurements

Measurements of burned tissue were performed by placing the skin sample on a tray and raising it into contact with the imaging window. SFDI was performed on the center of each skin sample. Immediately after imaging, the skin was removed from the system and biopsied. The biopsy was taken from the middle of the imaging area.

Image analysis

For the SFDI analysis, 6 spatial frequencies were used (0 to 0.22 mm^{-1}). For each frequency, the three phases were demodulated in order to extract the spatially modulated

component of the diffuse reflectance (Cuccia et al., 2009). The reflectance data at each pixel were then fit to a Monte Carlo model to quantify absorption (μ_a) and reduced scattering (μ_s'). The Monte Carlo method was chosen instead of the diffusion approximation due to the high tissue absorption (Bodenschatz et al., 2014). This process was repeated at each wavelength and for each burn duration. Tissue scattering was modeled as Mie type behavior, $\mu_s' = A\ (\lambda/\lambda_0)^{-b}$ where λ_0 is the normalization wavelength (700 nm), the parameter A characterizes the magnitude of scattering and b characterizes the wavelength dependence, related to scattering power (Mourant et al., 1997). Both A and b were determined using a nonlinear algorithm (lsqnonlin, Matlab) to fit the scattering at each pixel to the Mie model.

Histology

After optical measurements, 6 mm punch biopsies were taken from the center field of view. The tissue was subjected to a one-hour treatment with formalin, and stored in 70% ethanol. The biopsies were inked, serially sectioned, and entirely submitted for processing. Following processing, the tissue was paraffin-embedded, cut into 5 micron thick sections, and stained with hematoxylin and eosin. Biopsies were imaged with light microscopy to assess for thermal injury and read independently by two dermatopathologists in a blinded fashion (SK, TO). The depth of injury was measured in millimeters from the basement membrane to the deepest extent of the dermal connective tissue alteration using an ocular micrometer. Values are reported as the mean and standard deviation.

Results

Thermal burn injury results in reproducible skin damage

Four human skin samples were treated *ex vivo* with either a 10 second or a 60 second thermal injury (Fig 1a). As shown in Figure 2, the thermal injury resulted in distinct histologic changes including epidermal blistering and swelling/degradation of dermal collagen. The depth of dermal damage was easily visualized using hematoxylin and eosin staining. The control sample (Fig. 2a) showed no damage while the 10 and 60 second burn samples (Fig 2b–d) showed noticeable damage. As noted in Fig 2d, the 60 second injury resulted in full dermal damage. Measuring the distance from the basement membrane to the extent of the damage resulted in values of 1.15 ± 0.07 mm for the 10 second injury and 4.1 ± 0.5 mm for the 60 second injury (mean ± SD; N = 4). These findings indicate that our injury model results in a reliable damage response.

SFDI provides quantitative optical property maps

Representative optical property maps from one sample are shown in Figure 3a and 3b. Both the 10-sec and 60-sec burns showed changes in absorption and scattering parameters compared to control. At all four wavelengths, the absorption increased with burn duration, while scattering increased for 490 nm and decreased at the other wavelengths. Figures 4a and 4b summarize the wavelength dependency of the absorption and scattering parameters respectively. Absorption was >4x higher for the long burn duration compared to control skin at 490 nm (13.23 ± 8.03 vs. 3.02 ± 1.74, p = 0.03) and >8x higher at 780 nm (1.01 ± 1.22 vs. 0.12 ± 0.11, p = 0.03). Scattering was not significantly different at any wavelength. Significance was determined with the Wilcoxon rank sum test.

Burn depth measured with histology correlated with scattering power parameter

We then obtained the maps of A and b in the scattering parameters by using the multi-wavelength information. Figure 5 shows the maps of A and b for the same sample shown in Figure 3. Due to the large difference in depth of penetration (and therefore interrogation volume) the 490 nm measurement was excluded from the multi-wavelength analysis. As Figure 6a shows, the scattering parameter b correlated very well with the burn depth measured by histological analysis for all samples. The results indicate that the deeper the burn the higher the value of the b parameter. Additionally, Figure 6b shows the scattering power parameter was sufficient to fully characterize (100% sensitivity, 100% specificity) the burn severity characterized by the burn depth.

Discussion

Thermal injury is a clinically important problem associated with considerable morbidity and even mortality (Miller et al., 2007). One important need in this field for the clinician is to rapidly discern the burn depth, since a deeper burn would necessitate more aggressive treatment including fluid resuscitation and skin grafting (Miller et al., 2007, Renz and Cancio, 2012, Tiwari 2012). We built a fast, clinic-friendly SFDI system to test whether this methodology could have use for early assessment of burns. The advantages of this system include that it is non-invasive, and can rapidly assess thermal burn injury depths. This technology could also be adapted to a hand-held instrument that would allow easy use in the field.

Measurements were taken on *ex vivo* tissue so hemoglobin is expected to contribute little to the overall tissue absorption. Burns *in vivo* will alter the vasculature and hemodynamic changes (such as total hemoglobin concentration [THC] and tissue oxygen saturation [StO_2]) and will provide an additional source of contrast for burn depth estimation (Mazhar et al., 2014). Yet, our findings correlate nicely with those of porcine skin *in vivo*, suggesting the utility of this *ex vivo* model of thermal burn injury of human skin. Ultimately this model could be adapted for use in other environmental injuries to include caustic agents and vesicants to minimize the use of live animals in these types of studies.

Acknowledgments

This research was supported in part by grants: the Ohio Third Frontier to the Ohio Imaging Research and Innovation Network (OIRAIN, 667750), the National Institutes of Health grants HL062996 (JBT), ES020866 (JBT), AG048946 (JBT), AR070010 and Veteran's Administration Merit Award (JBT).

References

Bodenschatz N, Brandes A, Liemert A, Kienle A. Sources of errors in spatial frequency domain imaging of scattering media. J Biomed Opt. 2014; 19:071405.doi: 10.1117/1.JBO.19.7.071405 [PubMed: 24474551]

Cuccia DJ, Bevilacqua F, Durkin AJ, Ayers FR, Tromberg BJ. Quantitation and mapping of tissue optical properties using modulated imaging. J Biomed Opt. 2009; 14:024012.doi: 10.1117/1.3088140 [PubMed: 19405742]

Cuccia DJ, Bevilacqua F, Durkin AJ, Tromberg BJ. Modulated imaging: quantitative analysis and tomography of turbid media in the spatial-frequency domain. Opt Lett. 2005; 30:1354–1356. [PubMed: 15981531]

Gioux S, Mazhar A, Lee BT, Lin SJ, Tobias AM, Cuccia DJ, Stockdale A, Oketokoun R, Ashitate Y, Kelly E, Weinmann M, Durr NJ, Moffitt LA, Durkin AJ, Tromberg BJ, Frangioni JV. First-in-human pilot study of a spatial frequency domain oxygenation imaging system. J Biomed Opt. 2011; 16:086015.doi: 10.1117/1.3614566 [PubMed: 21895327]

Mazhar A, Saggese S, Pollins AC, Cardwell NL, Nanney L, Cuccia DJ. Noncontact imaging of burn depth and extent in a porcine model using spatial frequency domain imaging. J Biomed Opt. 2014; 19:086019.doi: 10.1117/1.JBO.19.8.086019 [PubMed: 25147961]

Miller SF, Bessey P, Lentz CW, Jeng JC, Schurr M, Browning S, Committee AN. National burn repository 2007 report: a synopsis of the 2007 call for data. J Burn Care Res. 2008; 29:862–870. discussion 871. DOI: 10.1097/BCR.0b013e31818cb046 [PubMed: 18997556]

Mourant JR, Fuselier T, Boyer J, Johnson TM, Bigio IJ. Predictions and measurements of scattering and absorption over broad wavelength ranges in tissue phantoms. Appl Opt. 1997; 36:949–957. [PubMed: 18250760]

Muldoon TJ, Burgess SA, Chen BR, Ratner D, Hillman EM. Analysis of skin lesions using laminar optical tomography. Biomed Opt Express. 2012; 3:1701–1712. DOI: 10.1364/BOE.3.001701 [PubMed: 22808439]

Nguyen JQ, Crouzet C, Mai T, Riola K, Uchitel D, Liaw LH, Bernal N, Ponticorvo A, Choi B, Durkin AJ. Spatial frequency domain imaging of burn wounds in a preclinical model of graded burn severity. J Biomed Opt. 2013; 18:66010.doi: 10.1117/1.JBO.18.6.066010 [PubMed: 23764696]

Nguyen TT, Ramella-Roman JC, Moffatt LT, Ortiz RT, Jordan MH, Shupp JW. Novel application of a spatial frequency domain imaging system to determine signature spectral differences between infected and noninfected burn wounds. J Burn Care Res. 2013; 34:44–50. DOI: 10.1097/BCR.0b013e318269be30 [PubMed: 23292572]

Ozturk MS, Chen CW, Ji R, Zhao L, Nguyen BN, Fisher JP, Chen Y, Intes X. Mesoscopic Fluorescence Molecular Tomography for Evaluating Engineered Tissues. Ann Biomed Eng. 2016; 44:667–679. DOI: 10.1007/s10439-015-1511-4 [PubMed: 26645079]

Ponticorvo A, Burmeister DM, Yang B, Choi B, Christy RJ, Durkin AJ. Quantitative assessment of graded burn wounds in a porcine model using spatial frequency domain imaging (SFDI) and laser speckle imaging (LSI). Biomed Opt Express. 2014; 5:3467–3481. DOI: 10.1364/BOE.5.003467 [PubMed: 25360365]

Renz EM, Cancio LC. Acute Burn Care. In: Savitsky E, Eastridge B, editorsCombat Casualty Care: Lessons Learned from OEF and OIF. Office of the Surgeon General; United States of America: 2012.

Rohrbach DJ, Muffoletto D, Huihui J, Saager R, Keymel K, Paquette A, Morgan J, Zeitouni N, Sunar U. Preoperative mapping of nonmelanoma skin cancer using spatial frequency domain and ultrasound imaging. Acad Radiol. 2014; 21:263–270. DOI: 10.1016/j.acra.2013.11.013 [PubMed: 24439339]

Rohrbach DJ, Zeitouni NC, Muffoletto D, Saager R, Tromberg BJ, Sunar U. Characterization of nonmelanoma skin cancer for light therapy using spatial frequency domain imaging. Biomed Opt Express. 2015; 6:1761–1766. DOI: 10.1364/BOE.6.001761 [PubMed: 26137378]

Thatcher JE, Squiers JJ, Kanick SC, King DR, Lu Y, Wang Y, Mohan R, Sellke EW, DiMaio JM. Imaging Techniques for Clinical Burn Assessment with a Focus on Multispectral Imaging. Adv Wound Care (New Rochelle). 2016; 5:360–378. DOI: 10.1089/wound.2015.0684 [PubMed: 27602255]

Tiwari VK. Burn wound: How it differs from other wounds? Indian J Plast Surg. 2012; 45:364–373. DOI: 10.4103/0970-0358.101319 [PubMed: 23162236]

Yafi A, Vetter TS, Scholz T, Patel S, Saager RB, Cuccia DJ, Evans GR, Durkin AJ. Postoperative quantitative assessment of reconstructive tissue status in a cutaneous flap model using spatial frequency domain imaging. Plast Reconstr Surg. 2011; 127:117–130. DOI: 10.1097/PRS.0b013e3181f959cc [PubMed: 21200206]

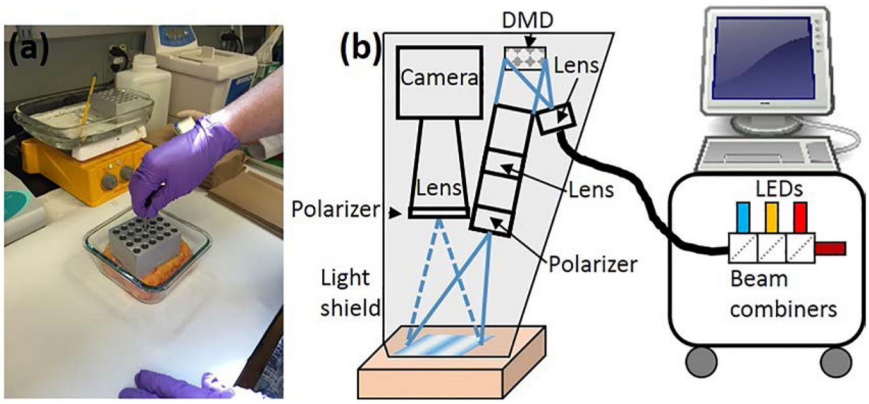

Figure 1.
(a) Picture of skin undergoing thermal burn injury. (b) Schematic of setup

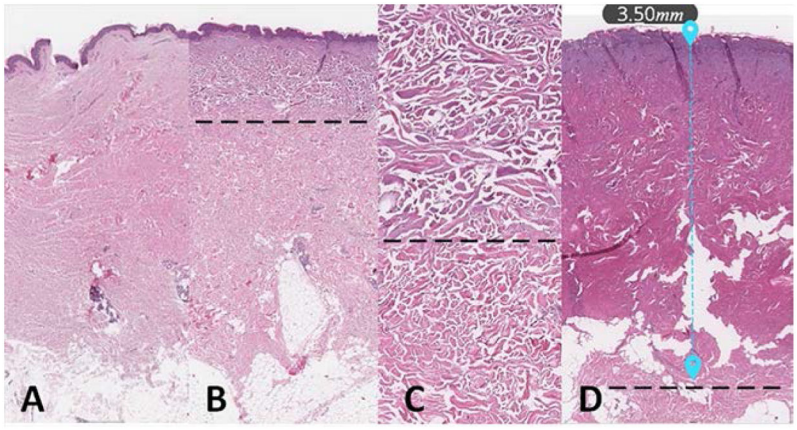

Figure 2.

Burn depth assessed with histology. (a) Control; (b) 10 second burn; (c) High-power view of dermis in the 10 second burn; (d) 60 second burn. Dotted lines denote changes in collagen indicating burn depth.

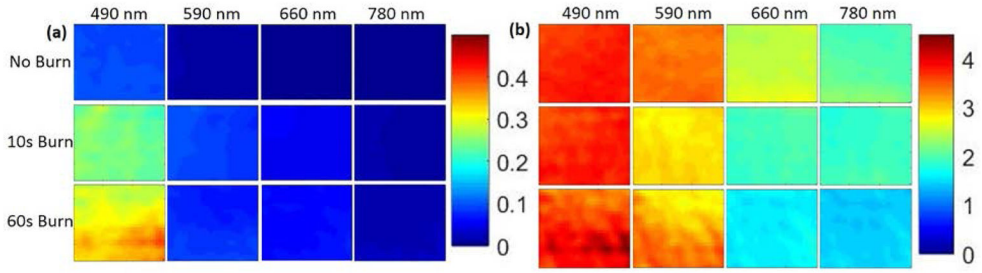

Figure 3.
Optical property maps for one sample. (a) Absorption and (b) Scattering

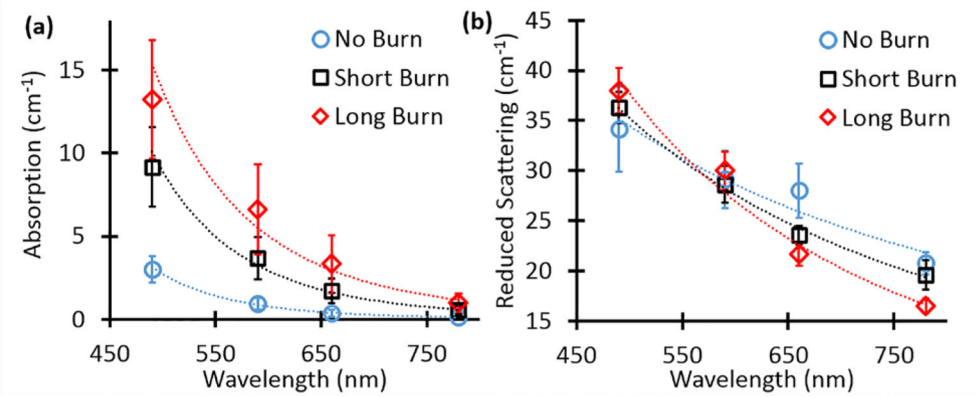

Figure 4.

Optical properties for all samples. (a) Absorption as a function of wavelength for each burn duration. (b) Reduced scattering as a function of wavelength for each burn duration. Error bars are the standard error for all samples.

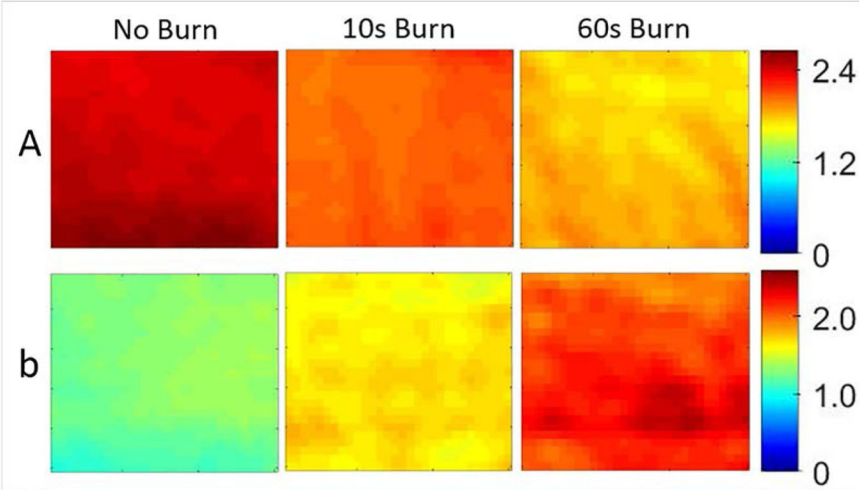

Figure 5.
Multi-wavelength fitting results for scattering parameters A and b for one sample.

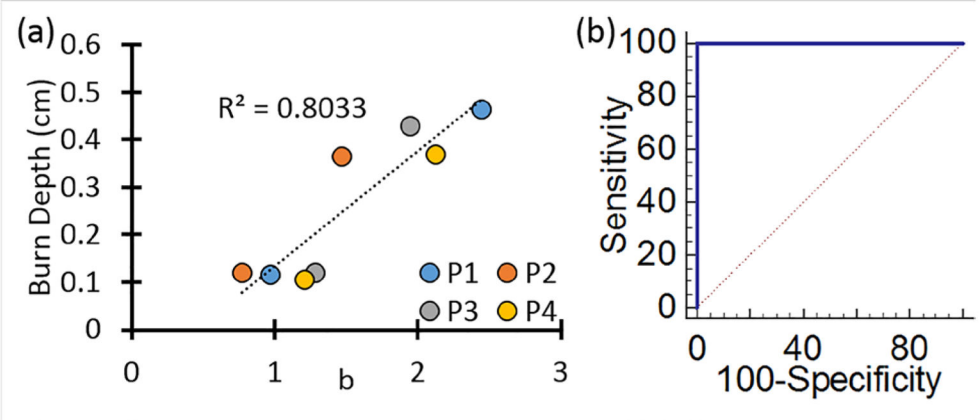

Figure 6.

(a) Correlation with burn depth vs scattering power parameter b for each subject. (b) Sensitivity-specificity plot indicating full discrimination can be obtained by using this scattering parameter.